

Status Report of
Shielding Investigation in Japan

1 9 6 4 年 5 月

日本原子力研究所

Japan Atomic Energy Research Institute

Status Report of Shielding Investigation in Japan

Summary

Shielding studies, experimental and theoretical, which have been done in Japan till the beginning of 1964, are described in this report. Some computer codes developed in Japan are also described as well as the brief outline of the JRR-4.

Originally this report was prepared for and presented to the Panel on Reactor Shielding, which was held by IAEA at Vienna on 9 - 13, March, 1964.

April 1964

Shielding Laboratory
Tokai Research Establishment

日本における遮蔽研究の現状

要 旨

1964年初めまでに日本においておこなわれた遮蔽に関する実験的、理論的研究がこの報告書にのべてある。日本において開発された計算コードとJRR-4の簡単な概要も書かれている。

この報告書はIAEAの主催により1964年3月9日-13日にウィーンで開催された原子炉遮蔽に関するパネル会議のため作成提出されたものである。

1964年4月

東海研究所 遮蔽研究準備室

CONTENTS

1. INTRODUCTION	1
2. EXPERIMENTAL STUDIES	2
2.1 Gamma-Ray Shielding	
2.1.1 Penetration and Scattering	
2.1.2 Reflection	
2.1.3 Volume Source Shielding	
2.1.4 Streaming and Labyrinth	
2.2 Neutron Shielding	
2.3 Instrumentation	
3. THEORETICAL STUDIES	7
3.1 Transport and Monte Carlo Calculations	
3.2 Design Techniques	
3.3 Optimization	
4. COMPUTER CODES	12
5. FACILITIES FOR SHIELDING EXPERIMENTS IN JAPAN	14
5.1 Pool and its Experiment Facilities	
5.1.1 Pool	
5.1.2 Instrument Bridge	
5.2 Lid Tank Facility	
5.2.1 Lid Tank	
5.2.2 Thermal Column	
5.2.3 Converter	
5.2.4 Instrument Bridge	
5.3 Dry Shielding Test Facility	
5.3.1 Dry Shielding Test Room	
5.3.2 Beam Hole	
5.3.3 Gamma-ray Source Apparatus	
5.3.4 Instrument Bridge	
6. CONCLUSION	16
REFERENCES	17
FIGURES	20

目 次

1.	まえがき	1
2.	実験的研究	2
2.1	ガンマ線の遮蔽	
2.1.1	透過と散乱	
2.1.2	反 射	
2.1.3	体積線源の遮蔽	
2.1.4	ストリーミングと迷路	
2.2	中性子の遮蔽	
2.3	計測器	
3.	理論的研究	7
3.1	輸送理論とモンテカルロ計算	
3.2	設計法	
3.3	最適化	
4.	計算コード	12
5.	日本の遮蔽実験設備	14
5.1	プールおよび実験設備	
5.1.1	プール	
5.1.2	プール用測定ブリッジ	
5.2	リドタンク実験設備	
5.2.1	リドタンク	
5.2.2	サーマルカラム	
5.2.3	コンバータ	
5.2.4	リドタンク測定ブリッジ	
5.3	散乱実験設備	
5.3.1	散乱実験室	
5.3.2	散乱実験孔	
5.3.3	ガンマ線源装置	
5.3.4	散乱実験用測定ブリッジ	
6.	あとがき	16
文	献	17
図	20

1. INTRODUCTION

Ten years have passed since the peaceful use of nuclear energy started in Japan. The Japan Atomic Energy Research Institute (JAERI) was established in 1954, and immediately proceeded with the construction of a research reactor. Operation was initiated in every field of nuclear research, but the shielding study was for long only a small part of health physics activities, incorporating such a small group of research workers that they could not properly organize their activities. In 1957 was held the first symposium in Japan on nuclear energy. Most of the papers presented in the branch of reactor shielding were limited to shielding materials and their fabrication. In the first stage of our investigations, our efforts were devoted to practical design studies of reactor shielding. As a result of these studies, it was found that formulas at hand for calculations were not adequate, but at that time no electronic computer was available in Japan nor were theoretical calculations very actively undertaken.

Problems on nuclear ship shielding were being investigated at the Ship Research Institute, former the Transportation Technical Research Institute, since 1956, and many fruitful results had been obtained. About that time the Japan Atomic Industry Forum started activities and took the initiative in organizing shielding research. Research workers in the shipbuilding industry in particular have been seriously studying shielding problems.

Few years after the first symposium, problems concerning more fundamental studies came to be treated by many researchers. Shielding experiments using radio-isotopes were carried out and many fruitful results were obtained. They are described in the next chapter. Medium size electronic computers became available in Japan, which permitted a theoretical study group to make an active contributions. They (the SCG-group) produced some codes, sponsored by the Nuclear Powered Ship Research Association of Japan, and their results are described also in the following chapters. This constituted the second stage of our investigations.

JRR-4 (Japan Research Reactor-4), of swimming pool type, is now under construction at JAERI since 1962, and it will become critical this autumn. After characteristic tests, it will be a very powerful tool for the shielding investigations. We are now entering the third stage of our investigations.

2. EXPERIMENTAL STUDIES

2.1 Gamma-Ray Shielding

2.1.1 Penetration and Scattering

The most important data for gamma-ray penetration calculations are buildup factors. Miyasaka et al.¹⁾ obtained dose buildup factors of eight materials (water, graphite, ordinary glass, aluminum, ordinary concrete, heavy concrete, iron, and lead) for ^{60}Co plane monodirectional sources using a long ionization chamber²⁾ and with the same method as that developed by F. S. Kirn et al.³⁾. The data were compared with the theoretical values (except graphite, glass, and concrete) by the moments method using the Berger's finite effect correction and the results showed good agreement within 19% up to 7 mean free paths for all these materials except water. For water, the discrepancy was about 37% for 7 mean free paths. To trace the origin of this discrepancy, another calculations by Monte Carlo method were performed, and the result supported the calculated values.

The same experiment was made by Tamura et al. for ^{137}Cs plane monodirectional sources⁴⁾, and Monte Carlo calculations are also in progress.

Many experimental studies of buildup factors have been made for point isotropic sources and plane monodirectional sources, but there are few studies covering plane isotropic sources. Using the long ionization chamber and a point isotropic source, gamma-ray penetration study has been made for plane distributed isotropic sources by Tsuruo and Toyota⁵⁾. The sources used were ^{198}Au (0.412 MeV), ^{137}Cs (0.662 MeV), ^{60}Co (1.17 MeV and 1.33 MeV), and ^{24}Na (1.37 MeV and 2.75 MeV). Aluminum, iron, and lead were used for shielding material, with selected thicknesses up to 8 mean free paths. The dose rate distribution obtained experimentally was extrapolated by calculation to the case of infinite plane isotropic sources. The difference in value between limited plane sources and infinite plane sources was less than 3%. From these results, gamma-ray attenuation curves and dose buildup factors were obtained for infinite plane isotropic sources.

As a part of the gamma-ray penetration studies mentioned above, Kanemori et al. obtained dose buildup factors of multi-layers⁶⁾. Experiments were performed for the combinations of lead-iron, lead-aluminum, and lead-ordinary concrete for ^{60}Co plane monodirectional sources. The composite shielding was arranged in a variety of sequences, such as lead-iron, iron-lead, and iron-lead-iron-lead.

Typical results are shown in Fig. 1 for the effect of the difference in arrangement of heavier and lighter material.

Other investigations on multi-layers of water, iron, and lead for ^{60}Co plane monodirectional sources were performed by Mochizuki et al.^{7),8),9)} using the same method as F. S. Kirn et al.

In the investigations, an empirical formula was proposed. The formula enables quick and easy calculation of buildup factors for multi-layers composed of an arbitrary combination of materials, by using known buildup factors for finite mono-layers of the materials included in the composition.

Experimental results indicate that the buildup factors agree well with theoretical values for monolayers of iron and lead, and multi-layers

of the materials investigated in the case of relatively thin lead thickness, but not for water and multi-layers with thick lead portion.

Furthermore, experiments were performed for buildup factors of relatively thick lead multi-layers, and comparison was made between the experimental and theoretical results calculated from the generalized Kalos's formula¹⁰⁾ and from an empirical formula derived during the investigation. The results showed good agreement with theoretical values for iron-lead multi-layers, but not for lead-iron multi-layers with very thick lead layers.

Dose buildup factors of iron slabs for ^{60}Co and ^{137}Cs infinite line sources were obtained by Umeda experimentally¹¹⁾. Furthermore, experiments were performed to obtain dose buildup factors of steel pipes for ^{60}Co and ^{137}Cs isotropic line sources placed on the center axis of the pipe.

Aimed at obtaining the scattering of reactor gamma-rays, Nakata et al. measured gamma-ray dose rate distribution in water to which were introduced radiations from a beam hole of the reactor JRR-1¹²⁾. The results were compared with those from attenuation calculations using the energy spectrum obtained by Furuta and Tanaka¹³⁾ with a multiple-crystal gamma-ray spectrometer, and good agreement was obtained.

Ishimatsu¹⁴⁾ obtained the energy flux and dose rate distributions of gamma-rays from a point source of ^{60}Co in an infinite water medium. The experimental results were compared with calculated results by the moments method. A satisfactory agreement with calculations was obtained for the dose buildup factors given by the experimental results. On the other hand, a slight discrepancy seemed to exist between the experimental and the calculated energy flux spectra.

In the pool type reactors, it is generally considered that ^{24}Na atoms in the water contribute mostly to the gamma-ray dose on the water surface of the reactor. To determine this quantitatively for the case of TRIGA Mark II reactor (St. Paul's University), Hattori et al. have been measured the attenuation of gamma-rays in the shielding water of the reactor tank¹⁵⁾. The results were compared with calculated values, and good agreements were obtained. Furthermore, the gamma-ray spectrum in the water was obtained using nuclear emulsions soaked with heavy water.

2.1.2 Reflection

Experimental study on the gamma-ray backscattering has been made by Nakata et al. Measurements were made on the energy distribution of backscattered gamma-rays by lead, iron, and ordinary concrete slabs using a ^{60}Co and a ^{137}Cs sources. The results showed that the backscattered rays from a concrete wall are made up from multi-scattered rays, while backscattered rays from a lead slab consist mainly of the singly scattered photons and the characteristic X-rays¹⁶⁾.

Furthermore, Kakata¹⁷⁾ measured backscattered gamma-rays with a lead plate placed on a concrete wall, and found that the lead plate markedly depressed the reflecting photon flux. Dose rates in a model room of which walls were covered with lead plates amounted to about one half of that of uncovered walls.

The backscattered gamma-rays from scatterers of paraffin, aluminum, iron, tin, and lead of thickness semi-infinite in effect were measured by Hyodo¹⁸⁾. Point isotropic sources of ^{60}Co and ^{137}Cs were placed on the front face of the scatterer, and a 3 in. diameter by 3 in. long NaI(Tl) scintillator was moved in a circle centered on the position of

the source. The energy and number albedos, the angular distribution of scattered energy and number of photons, as well as the energy distribution were obtained for each combination of gamma source and scatterer. Table 1 shows the value of the number and the energy albedo obtained in the experiments.

The backscattered gamma-rays from iron¹⁹⁾, and polyethylene²⁰⁾, aluminum, and lead scatterer were measured as a function of the scatterer thickness with geometry similar to that described above. The asymptotic value of the angular distribution approached very near the Monte Carlo values.

Reflection dose buildup factors for ⁶⁰Co plane monodirectional sources were obtained by experiment as well as by Monte Carlo calculations by Tsuruo and Miyazaki²¹⁾. For aluminum and lead, the two results showed good agreement, and furthermore, agreed also with data obtained by the U.S. National Bureau of Standards.

In the study, reflection dose buildup factors were obtained for ordinary concrete, heavy concrete, copper slag, and ordinary concrete coated with several kinds of paint containing oxides of lead, barium, and tin.

The effect of surface material on backscattered gamma- and X-rays were studied. For ¹³⁷Cs gamma-rays, backscattering from concrete seemed to be much decreased by covering with lead lamina but not so much with iron. Backscattering from lead might decrease a little by covering with tin. For 70 keV X-rays, the problem is complicated. Generally, materials of which the atomic number are about 22 and between 60 and 70 are useful for degradation of backscattered radiations. Lead-iron-titanium lamina placed on thick concrete or wood slab was effective²²⁾.

At present, the reflection dose buildup factors for plane isotropic sources of several isotopes have been obtained by Furuta and Tsuruo²³⁾.

2.1.3 Volume Source Shielding

As yet few experiments have been made of gamma-ray shielding for volume sources. Furuta and Kanemori have studied gamma-ray penetration problems for cylindrical sources.

The special feature of the experiments was the use of a large number of plastic spheres each containing in the center a ⁶⁰Co pellet. Many forms of cylinder were constituted by these plastic spheres, and their effect was analogous to the cylindrical sources of ⁶⁰Co aqueous solution.

Dose rates were also measured from bare cylindrical source and from the cylindrical source covered with a cylindrical shell of iron²⁴⁾.

2.1.4 Streaming and Labyrinth

No satisfactory estimates of radiation leakage through ducts have yet been made.

Takumi and Mitsui made experiments on thermal neutron streaming through ducts²⁵⁾. The ducts were formed with 8 blocks of heavy concrete, 500 x 500 x 500mm, and their dimensions can be changed continuously.

Radiation leakage from pipes in water have been investigated in detail. The pipes are 16 - 200mm in inner diameter and 0 - 1500mm in length, and made of vinyl chloride, iron, lead, and aluminum. Investigations are planned for observing the effects of pipes and on the effect of substance like water in pipes²⁶⁾.

Sakuta made a series of measurements of gamma-ray distributions in entranceways of an irradiation facility, and showed how bends contributed to decreasing gamma-ray dose rate at the entrance²⁷⁾.

2.2 Neutron Shielding

Yamaki made experiments on neutron attenuation in layers of iron and water with 14 MeV neutrons produced by the $D(T,n)^4\text{He}$ reaction with a Cockroft-Walton type accelerator. Dependence of removal cross sections on the thickness of iron was obtained²⁸).

Experiments have been made on attenuation of fast neutrons, thermal neutrons and gamma-rays in multi-layers of iron and water with neutrons from natural uranium converter²⁹), besides, neutron attenuation in lead and mesonite were measured in the beam hole of a water boiler type reactor (JRR-1) by Tomabechi and Ishii³⁰).

2.3 Instrumentation

Information on gamma-ray spectrum penetrating through shielding materials is very important for the investigation of shielding problems. Many attempts have been made for measuring such continuous gamma-ray spectra with a single crystal. Ishimatsu³¹) developed a simple method to obtain the corrected gamma-ray spectrum, and made a response matrix for a 2 in. long by 2 in. diameter NaI(Tl) crystal using the method. It is applicable to broad parallel gamma-rays up to 1.5 MeV, and its application to the incident gamma-rays of uniform angular distribution has also been discussed.

Hyodo has been studying the response matrix for a 3 in. long by 3 in. diameter NaI(Tl) crystal for the purpose of obtaining response-corrected spectra of scattered gamma-rays³²). The matrix was made for axial incident gamma-rays having energies ranging from 0 to 1.440 MeV.

Another method of gamma-ray spectrometry has been developed by Furuta. It is a scintillation spectrometer based on the multiple-crystal gamma-ray spectrometer by F. C. Maienschein³³).

A trial model of the spectrometer was used five 1 in. long by 1 in. diameter NaI(Tl) crystals³⁴), and recently, it is envisaged to use 19 crystals (1 in. long by 1 in. diameter each) or ring type crystals for the purpose of increasing the efficiency³⁵).

On account of its response being expressible in roentgens, the ionization chamber with air equivalent wall, is widely used for gamma-ray dosimetry. Ionization chambers, however, have rather low sensitivity, and to raise it a large active volume or high pressure is required. Therefore, ionization chambers are not suitable for such applications as dose measurement in an area of low level gamma-rays outside thick shields or streaming radiations from ducts.

A gamma-ray dosimeter, which has a response expressible in roentgens and high sensitivity with a small sensitive volume, was perfected by Furuta and Kinbara³⁶). This dosimeter (Gamma-Ray Pulse Dosimeter) employs a plastic scintillator and a special electronic technique which involves no counting loss, and even with a 5mm long by 5mm diameter scintillator, natural background radiations could be measured. Fig. 2. shows the sensitivity of this dosimeter for several sizes of scintillators. The Gamma-ray pulse dosimeter is sensitive to X- or gamma-rays with energies above 50 keV, and have air equivalent response for energies above 200 keV, with maximum response at 80 keV (+14%). Furthermore, a linear temperature dependency is obtained (0.6 %/°C) under 40°C.

As neutron spectrometer for shielding experiments, the detector must have a high efficiency and be insensitive to gamma fluxes. The

threshold detector is insensitive to high gamma fluxes. The minimum neutron fluxes that can be measured by the threshold detector was calculated, and a revised orthonormal expansion method, minimizing the mean square relative deviation, was proposed by Fuse to obtain the fast neutron spectrum³⁷⁾.

Threshold detectors, however, are a rather rough device for neutron spectroscopy.

For precise measurements of the neutron spectrum, a proton recoil neutron spectrometer is in preparation by Furuta and Fuse³⁸⁾. It will be used for the spectrum measurements of the JRR-4 core neutrons.

In the mixed radiation field of gamma-ray and neutrons, scintillation detector usually respond to both radiations. Therefore, it is necessary to discriminate neutrons from gamma-rays in the neutron experiments on reactor shielding. Fuse³⁹⁾ has tried to find the optimum conditions for the discrimination of neutrons from gamma-rays using a method similar to that of Owen⁴⁰⁾. Several types of photomultipliers were examined for this purpose, and the results showed that the degree of discrimination depend on the type of photomultiplier tube. A clue for the mechanism of scintillation in anthracene is also suggested, that is, there may be some difference between the spectra of the fast and slow components of the light of scintillation, both of which are distributed around 4,000 Å.

Table 1. The Number Albedo A and the Energy Albedo A_E

Scatterer	Number albedo A		Energy albedo A _E	
	¹³⁷ Cs	⁶⁰ Co	¹³⁷ Cs	⁶⁰ Co
Paraffin	0.57 ± 0.02	0.46 ± 0.02	0.19 ± 0.01	0.112 ± 0.005
Aluminum	0.59 ± 0.02	0.52 ± 0.02	0.20 ± 0.01	0.136 ± 0.005
Iron	0.42 ± 0.02	0.42 ± 0.02	0.16 ± 0.01	0.120 ± 0.005
Tin	0.22 ± 0.02	0.25 ± 0.02	0.10 ± 0.01	0.088 ± 0.005
Lead	0.09 ± 0.02	0.17 ± 0.02	0.04 ± 0.01	0.059 ± 0.005

3. THEORETICAL STUDIES

3.1 Transport and Monte Carlo Calculations

Theoretical study of shielding in Japan started with the design of JRR-3. In the shielding design calculation for this research reactor undertaken from 1956 to 1957, the gamma-ray buildup factors of magnetite concrete was calculated by the moments method⁴¹⁾. An electronic computer suited for these calculations was not at hand in Japan at that time, so the IBM-602A and hand calculation were applied.

The Monte Carlo method has become the matter of interest of many investigators since the application of the electronic computer became possible. Tsuruo and Sibuya⁴²⁾ tried the Monte Carlo calculation by using the correlated sampling and expected value method for the gamma-ray transmission and reflection problems. They verified Berger's expectation⁴³⁾ by showing the fact that the ratio of gamma-ray transmission at the corner of a semi-infinite quadrant to corresponding penetration in semifinite medium became constant at a transmission distance of 2 - 3 mfp. Let the transmission buildup factor of photon obliquely incident upon the corner of the quadrant be $B(\infty/4)$, and let the penetration buildup factor of photon obliquely incident upon the semi-infinite medium be $B(\infty/2)$, then

$$k = \frac{B(\infty/4)-1}{B(\infty/2)-1} \quad (3.1)$$

becomes constant. Fig. 3 shows the value of k in the case of photon of energy 1.25 MeV when the incident angle is 45° , the medium being aluminum.

Toyoda and Kondo⁴⁴⁾ tried the bias sampling technique in order to calculate fast neutron penetration in water. Since 1962, codes for gamma-ray penetrations in slabs and multiple layers have been developed and compared with experiments of gamma-ray buildup factors. Calculations of transmission in a sphere and a cylinder were also made by Umeda⁴⁵⁾. Conditional Monte Carlo technique is now a matter of interest. Nakano⁴⁶⁾ tried to apply this technique in the gamma-ray problem in double-layer penetration. Monte Carlo calculations on complicated geometries have been tried by several investigators⁴⁷⁾, but meaningful results have not yet been obtained owing to computer speed limitation. Semi-analytic Monte Carlo calculation on streaming through ducts is now planned⁴⁸⁾ and good results are expected.

A new approach, the Response Matrix Method, to compute the transmission and reflection of gamma-rays in multi-layer slab shields has been developed by Kataoka⁴⁹⁾. In this method, response matrices are evaluated for two different thicknesses of each material slab, thin and thick, using the Monte Carlo method. The angular and energy spectra of transmitted and reflected gamma-rays in the given multilayer shield are calculated by operating these two sets of response matrices prepared for each elementary slab successively to the incoming gamma-rays. In the Response Matrix Method, the three kind of response matrices, i.e. the number current, the energy current and the energy flux, are evaluated at the same time by a Monte Carlo calculation. The examples of buildup factors in the case of water-lead multilayer shield are shown in Fig. 4,

and those are not of "energy flux" but of "energy current". The energy flux buildup factors computed by the Response Matrix Method agree well with the results of other Monte Carlo calculations and experiments. Those figures will be illustrated in the reference⁴⁹⁾. Each buildup factor in the figure is not the value at an inside point of such multiple layers, but is one at the boundary of layers of that thickness. This method determines the energy and angular distributions of gamma-rays in short machine time.

Direct numerical integration of the transport equation has become a matter of interest. A numerical integration code of transport equation for slab geometry, EOS, has been developed by Kataoka and Takeuchi⁵⁰⁾ for the NEAC 2206 computer. Some of the results obtained by EOS-1 code, code for gamma-ray calculation are shown in Fig. 5. Buildup factors deduced from these results coincide well with other calculations by moments method and Monte Carlo method. EOS-2 is the code for neutron calculation.

A numerical integration code of Boltzmann equation for spherically symmetrical geometry, NIOBE, originally devised for IBM 704 and 7090, has been prepared by Kataoka and Takeuchi for the NEAC 2206 computer⁵¹⁾. Several points to be borne in mind in applying the NIOBE to practical problems have been revealed.

3.2 Design Techniques

Scientists and engineers have been interested in developing simple and exact approximate formulas for design calculations. Ono and Tsuruo⁵²⁾ have devised refined approximate calculation methods for slab shielding to a volumetric source. These are based on the replacement of orthodox source geometry by other suitable geometry: A sphere is replaced by a partial spherical shell, and a cylinder by a partial cylindrical shell. Thus the integration is simplified and reduces error.

The geometrical effects of shields were investigated by Tsuruo⁵³⁾. For a spherical or cylindrical source, four kinds of shields, shown in Fig. 6 were investigated. On unscattered flux ϕ at point P, the following relation was obtained:

$$\phi_a \geq \phi_b \geq \phi_c \geq \phi. \quad (3.2)$$

Formulas expressing ϕ_a , ϕ_b and ϕ_c were obtained as also their approximate formulas. Ratios of ϕ_a to ϕ_b and ϕ_c , and geometrical effect functions, were calculated for the spherical and cylindrical sources. In Fig. 7 are shown the geometrical effect functions for spherical geometry, corresponding to Fig. 7.1 and 7.2 respectively, $S_1(x_0/R_0, \mu t)$ and $S_2(x_0/R_0, \mu t)$.

For neutron transmission calculation, Kataoka⁵⁴⁾ made a theoretical consideration of the combination of the effective removal theory and the diffusion equation. The three group theory, in which the first group is the thermal flux, is relatively simple and useful for application to multiple layers of water and metal. The upper limit of the second group has been obtained by trial and error in such manner as to make experimental results agree with the calculated one. Kataoka obtained the upper limit of the second group from theoretical consideration of neutron diffusion in water combined with the experimental results on LIDO by Cooper⁵⁵⁾. In like manner, a method was found of obtaining the

diffusion length and other constants of the second group, which agreed well with experimental results.

The expression for the intensity of gamma radiation which is generated in an infinite slab shield due to thermal neutron capture and escapes across the front and rear faces of the material is obtained by Hokkyo and Kitazume⁵⁶⁾ for given fast and thermal neutron currents incident on the shield. The result is based on the two group diffusion approximation for the thermal neutron distribution and is a natural extension of Iliffe's result⁵⁷⁾ which does not take the incident fast neutrons into account. Another expression is obtained for the case of water shield based on a fast removal group theory in connection with a thermal group diffusion equation, and the calculated intensities differ about 40% between the two expressions.

Approximate calculations of gamma-ray transmission in multiple layers have also been a subject of study. Mochizuki and Tanaka⁵⁸⁾ extended Kalos's formula⁵⁹⁾ on buildup factors of water and lead lamination taking into account the results of their gamma-ray experiments on multiple layers. They proposed approximate formulas for buildup factors of double layers other than water and lead laminas, and of four and six layers of double laminas of water and iron.

Comparing Broder's formula⁶⁰⁾ for buildup factors of multiple layer for a point isotropic source with Kalos's formula for vertically incident gamma-ray on a plane and with the results of Mochizuki's experiment, a revised Broder's formula for vertically incident gamma-ray on a plane was proposed by Kitazume⁶¹⁾:

$$B(\mu_1 X_1, \mu_2 X_2, \dots, \mu_N X_N) = B_N(\mu_1 X_1 + \dots + \mu_N X_N) + \{B(\mu_1 X_1, \dots, \mu_{N-1} X_{N-1}) - B_{N-1}(\mu_1 X_1 + \dots + \mu_{N-1} X_{N-1})\} e^{-\alpha \mu_N X_N} \quad (3.3)$$

where $B(\mu_1 X_1, \dots, \mu_N X_N)$: buildup factor of N layers of slabs, the thickness of the i -th slab being $\mu_i X_i$

$B_N(\mu_1 X_1, \dots, \mu_N X_N)$: buildup factor of the N -th slab

The buildup factor of N layers can be obtained by iteratively applying the results for a single layer. Depending on the materials, α must be determined empirically.

Tsuruo⁶²⁾ proposed a kind of matrix method for transmission in multiple layers. The differential energy spectra of transmitted gamma-ray from a slab of single material of thickness t are

$$I_1^D(E) = I(E) e^{-\mu(E)t}$$

$$I_1^S(E) = \int_E^{E_{max}} I_1^D(E') B_E(E', t) k(E', t) \psi(E' \rightarrow E, t) dE' \quad (3.4)$$

$$I_1(E) = I_1^D(E) + I_1^S(E)$$

where I^D : unscattered gamma-ray in the slab
 I^S : scattered gamma-ray in the slab
 $\mu(E)$: attenuation coefficient
 $B_E(E, t)$: energy buildup factor in infinite medium
 $k(E, t)$: Berger's finite slab effect coefficient

$\psi(\mathbf{E}' \rightarrow \mathbf{E}, t)$: probability density of scattering in which energy of a photon changes from \mathbf{E}' to \mathbf{E}

$$\int_{\mathbf{E}'} \psi(\mathbf{E}' \rightarrow \mathbf{E}, t) d\mathbf{E} = 1$$

If scattered gamma-rays are assumed to travel vertically from the slab after transmission, (3.4) can be applied to multiple layers. It is convenient to express (3.4) in the form of matrix. The incident differential energy flux is expressed by a vector, and the shielding properties of each slab of the multiple layer are expressed by a series of matrices. These matrices can be constructed by a relatively simple procedure, using the data of penetration in infinite medium calculated by the moments method and the data of the effect of a finite slab calculated by the Monte Carlo method. The results of the method are compared with those of the Monte Carlo calculation for Pb-H₂O and H₂O-Pb stratified slabs, and also with those of experiments for Pb, Fe and Al stratified slabs. The comparison shows that this method is useful for all combinations of materials at high incident energy and when low energy gamma-rays enter the heavy layer followed by a light or heavy layer.

Some trials were made on duct streaming. Kitazume⁶³⁾ derived a formula extending Simon-Clifford's to the two group theory. If the length of a duct L is sufficiently long compared with its diameter the fast and thermal neutron fluxes are respectively expressed by

$$\begin{aligned} \phi_1 &= \frac{R_0^2}{2L^2} \phi_{10} \left\{ 1 + \beta_1 \left(1 + \frac{R_0}{L} \tan^{-1} \left(\frac{8L}{5R_0} \right) \right) \right\} \\ \phi_2 &= \frac{R_0^2}{2L^2} \phi_{20} \left\{ 1 + \left[\beta_2 + \left(\frac{\phi_{10}}{\phi_{20}} \right) \beta_{12} \right] \left(1 + \frac{R_0}{L} \tan^{-1} \frac{8L}{5R_0} \right) \right\} \end{aligned} \quad (3.5)$$

where ϕ_1 : fast neutron flux at the inlet of the duct
 ϕ_2 : thermal neutron flux at the inlet of the duct
 ϕ_1 and ϕ_2 are isotropic
 β_1 : albedo of fast neutron
 β_2 : albedo of thermal neutron
 β_{12} : albedo of fast neutron slowing down to thermal neutron and ϕ_{12} are expressed by the diffusion coefficient of neutron, diffusion length, slowing down length and combination coefficient of fast neutron and thermal neutron.

Shindo et al⁶⁴⁾ have systematically studied duct streaming. The radiation fluxes at the exit were divided into that from the inlet disc and that from the annular part surrounding it. Further, unscattered, single scattering and multiple scattering radiations were separately considered, and the contribution of each of them investigated. Interesting results on unscattered and single scattering cases were obtained.

A simple method was derived by Tagami and Kitazume⁶⁵⁾ to estimate the effects of gamma-ray scattering in the infinite air medium around the local shielding. They can readily obtain the mapping of gamma radiation dosage around local shielding by this method which is assumed the point source and single scattering of gamma-ray in air but involves the corrections for multiple scattering effect by utilizing the buildup factor. Compared with the measurements of gamma-ray distribution around

the Ozenji Critical Facility, it is shown that the method gives the reasonable features for air scattering of gamma-ray.

Kitazume and Tagami⁶⁶⁾ obtained the expressions for the primary neutron and gamma-ray attenuations in water of swimming pool reactor by utilizing a single removal group theory in connection with two-group diffusion equation for neutron attenuation and eight-group energy source for gamma-rays, and using a modified point source approximation for reactor core. The expression for the photoneutron distribution in water which is generated by photo-reaction with deuterium contained in natural water, is also obtained by introducing the source term of photoneutron into one-group neutron diffusion equation. Utilizing above expressions for neutron flux distribution, the expression for the captured gamma-ray distribution which are generated due to thermal neutron capture and thermal photoneutron capture are obtained. Compared with the experimental results of HTR in Hitachi and BSR in ORNL, it is shown that calculated neutron and gamma-ray distribution in the pool water are good agreement with the measurements in accuracy of approximately 30% over all positions in the water of seven meter depth.

3.3 Optimization

Tanaka et al⁶⁷⁾ investigated widely maritime reactor shield optimization with respect to weight. A formula on the weight of the maritime reactor shield, consisting of the weight of the shield of the reactor itself and auxiliary equipment, was derived with some assumptions. It is a function of the dimension of the reactor, power, temperature, pressure, enrichment of uranium and etc., and the changes of the weight of the shield were investigated changing parameters. As the weight of the secondary shield is a important part, its effect on the primary shield was widely investigated.

Tsuruo⁶⁸⁾ investigated the optimization with respect to a container shield and a exclusion distance concerning the accident of reactor on land. As Japan is densely populated and land is expensive, it is necessary to shield a container of a large scale reactor with concrete and to have an exclusion area around the reactor expecting accidents. The exclusion distance and the thickness of the shield supplement each other. When prices of concrete and land, the maximum permissible dose rate and constants on the geometry of the shield were given, a monograph was made for obtaining the optimum exclusion distance R , thickness of the wall of concrete t_1 , thickness of ceiling t_2 .

Some trials have also been made for obtaining optimum conditions for shielding facilities utilizing radiations except the reactor. Sakuta⁶⁹⁾ investigated the relation between position of target and volume of concrete of shield for a linear accelerator facility for the case that the target room is on ground, semi-underground and underground. Initial and running costs of air conditioning was investigated also.

Okajima⁷⁰⁾ investigated systematically the optimum shield for accelerators, considering economics and construction method.

4. COMPUTER CODES

The development of computer codes for shielding calculations in Japan was started in 1958 using a relay type computer, FACOM 128. The use of small size digital computers followed immediately after, such as the IBM 650 installed in JAERI and others, like USSC-90, NEAC 2203 and Bendix-GL5D.

In 1959 an active group of researchers and engineers from research institutes, universities and private organizations throughout Japan was established with the object of mutual collaboration in the development of computer codes for shielding calculations. This group, the Shielding Codes Group (SCG), has been completed thirty five computer codes related to almost all kinds of shielding design calculations including the following⁷¹⁾: neutron shield design, primary gamma shield design, secondary gamma shield design, estimation of coolant activity source intensity, calculation of fission product source intensity, evaluation of gamma-rays scattered by air and by wall, estimation of temperature distribution and thermal stress in a shield, evaluation of gamma-ray dose outside a reactor container in the event of fission product release accident, fundamental survey codes for computation of gamma-ray streaming through a cylindrical straight duct. In addition to SCG activities, JAERI, the Ship Research Institute, the University of Tokyo and several private organizations have also been working on the development of shield computer codes and have produced twenty nine codes, from 1959 to 1963.

Medium scale computers, such as IBM 7070, FACOM 222 and NEAC 2206, and three installations of large scale computers, all IBM 7090, have in recent years become available for shielding researchers and engineers. Among others, a NEAC 2206 computer was installed in the Ship Research Institute in 1962 especially for the purpose of developing marine reactor shielding evaluation techniques and of marine reactor hazard analysis. In 1964, an IBM 7044 has come into use at JAERI as a device for general research work.

Because there are so many codes produced, it would not be possible to explain all of them. Among the work done by SCG, the SCG-RAC code developed by Abe, Fukugaki, Hachiya, Komatsu, Nakano and Toyoda⁷¹⁾ for IBM 7090 is one of the most distinguished shielding design codes in Japan. It can handle the following four categories of shielding calculations for cylindrical source geometry with cylindrical shell shields in a single computer run in any sequence desired. REMOVAL computes energy dependent removal group neutron distributions in the shield up to eighteen energy groups. DIFFUSION is a neutron diffusion code with up to six energy groups. PRY.GAMMA calculates the gamma-ray fluxes in energy groups up to ten using a single buildup factor of each energy group defined throughout whole shield. SEC.GAMMA evaluates secondary gamma-ray flux distributions in the same manner as PRY.GAMMA but with source distribution determined by the thermal neutron flux of DIFFUSION. The SCG-RAC code also prepares the input data to the SCG-GH-N code by Fukugaki⁷¹⁾ for IBM 7090, which computes temperature distribution and thermal stresses in the shield.

To estimate gamma-ray source intensity by fission products accumulated in the core, a series of codes were prepared for IBM 650 and FACOM 222. They are SCG-FP-G, SCG-FP-B, SCG-FP-I and SCG-FP-B and I by Kikuchi, Toyoda, Hachiya, Miyamoto and Kuwashima⁷¹⁾. SCG-CA-F, SCG-CA-I and

SCG-CA-F by Mori and Nakano⁷¹⁾ for NEAC 2203 evaluate the coolant activities caused respectively by the induced activity of coolant itself, by the induced activity of impurities in the coolant and by the radiation of fission products which have leaked into coolant from fuel elements. Kitazume developed SCG-SCA-1 and SCG-SCA-2 for IBM 7090, which calculate the gamma-rays scattered from walls of both large and small sizes compared to the size of the incident beam width.

Taking consideration of ship structure, tanks, reactor plant container, plant components and shielding structures, a code was completed for the NEAC 2206 computer by Kataoka et al. The main features of the code, MARINE-1, are as follows. At first, the radiation sources can be treated as a sum of volume elementary sources and/or surface elementary sources up to two hundred. The angular distribution of source intensity can be expressed by the power series of the cosine of the angle to the direction which is defined arbitrarily at each source point. If desired, the angular distribution of each source intensity can be limited within the half space, i.e., no photon radiates in the half space chosen arbitrarily. The secondary, the buildup factors of gamma-rays obliquely incident to finite slabs are evaluated with the Response Matrix Method described in Chapter 3.

Besides shielding design codes, there are many other codes prepared with the view to research studies as well as to design work. The ETC code⁷²⁾, a numerical integration code of the transport equation for slab geometry, has been developed and described in Chapter 3. There are several Monte Carlo treatments of gamma-ray calculation. In the slab geometry, both KAZAK-II by Tsuruo⁷³⁾ for IBM 7090 and AMONTF by Nakano⁷⁴⁾ for 7090 treat gamma-ray multilayer problems. MC-MATRIX code by Kataoka⁴⁹⁾ for NEAC 2206 has been applied to prepare the matrices of each material for the Response Matrix method. NKM-1 and NKM-2 by Umeda for IBM 7070 compute gamma-ray behaviours in the spherical and cylindrical geometry shield.

MULTI-LAYER SYNTHESIS 2 by Kataoka⁴⁹⁾ for NEAC 2206 is a code to calculate gamma-ray spectrum transmitted and reflected from multilayer shields by means of the Response Matrix method mentioned in Chapter 3.

There are a series of codes which evaluate the gamma-ray streaming through straight cylindrical ducts. Among them, SCG-LGEL by Tsuruo for IBM 7090 calculates the unscattered and once scattered flux by means of numerical integration. SCG-SC-M1 by Shimamura⁷⁵⁾ for IBM 7090 evaluates gamma-ray flux and current using the Monte Carlo method in the same situation as above.

5. FACILITIES FOR SHIELDING EXPERIMENTS IN JAPAN

We have the Research Reactor-4 (JRR-4) at the Japan Atomic Energy Research Institute. It is now under construction and will become critical in October, 1964. It is an enriched-uranium fueled, water moderated and cooled, swimming pool type reactor. The normal operating power is 1,000 kW, the maximum power being 3,000 kW. In Figs. 8-10 are shown the floor plan, cross section and artist's sketch of JRR-4. As experimental facilities, JRR-4 is equipped with i) pool, ii) lid tank facility, iii) dry shielding test facility and iv) gamma-ray source apparatus.

5.1 Pool and its Experiment Facilities

5.1.1 Pool

The pool is separated by a gate into two parts, No. 1 pool and No. 2 pool. The former is for fundamental experiments with relatively small samples. The latter is for actual size experiments with large samples. No. 1 pool is of raised type, 7 meters wide, 7 meters long and 10 meters deep, water depth being 9.8 meters. All inside faces of the pool are lined with aluminum. There are a beam hole, a thermal column and an air rabbit tube in the three directions of the raised part. No. 2 pool is 7 meters wide, 9 meters long and 10.3 meters deep, water depth being 9.8 meters. It is lined with aluminum like No.1 pool. It has a well 3 meters wide, 4 meters long and 1 meter deep in the center, to provide a space free from the effects of wall scattering and induced activity, and allows also for the adjustment of sample height to align the sample with core center lines.

The reactor is operated with high power (above 200 kW) with core placed at the center of raised part of No. 1 pool and at a distance of 3 meters from the center of the gate in No. 2 pool. It is operated with low power near the high power position.

5.1.2 Instrument Bridge

The measuring instruments are hung from the instrument bridge that spans the pools in parallel to the reactor bridge. Two carts travel independently on a pair of rails on the bridge. A shaft, suspended from the cart, carries at its end the measuring instruments, which can be positioned at any point in the pool. The instrument bridge is operated from the control panel located at the corner of the bridge. The position of the instrument is shown by synchros with an accuracy of 1 mm.

5.2 Lid Tank Facility

5.2.1 Lid Tank

The lid tank is 4 meters wide, 4.5 meters long and 6.5 meters deep, water depth being 6.2 meters. It is lined with aluminum like the pool.

5.2.2 Thermal Column

The thermal column is placed between the lid tank and the reactor on the raised part of No. 1 pool. It is 4.36 meters long. The cross sections at the reactor side and the lid tank side are $50 \times 50 \text{ cm}^2$ and $1.2 \times 1.2 \text{ m}^2$ respectively. The thermal flux is expected to be above

10^8 n/cm²-sec at the outer end of the column.

5.2.3 Converter

The converter is a disk of uranium metal, 60 cm in diameter, of uranium enriched to 20% in ²³⁵U (3 kg of ²³⁵U). The power is expected to be about 10 W, though it would depend on the thermal flux from the thermal column.

5.2.4 Instrument Bridge

An instrument bridge, similar to that of the pool, spans the tank.

5.3 Dry Shielding Test Facility

The dry shielding test facility is for shielding experiments in the air.

5.3.1 Dry Shielding Test Room

The dry shielding test room is 14 meters long, 14.5 meters wide, 9.4 meters high. It is a semi-underground reinforced building, adjacent to the reactor room. It has a beam hole, a gamma-ray source apparatus and an instrument bridge. When experiments are carried out, personnel are not allowed in the room, and so the measuring instruments must be controlled from the measuring room adjacent to the test room, and monitoring is by closed circuit television and through a shielding window.

5.3.2 Beam Hole

The beam hole penetrates the wall, 3 meters thick, between No. 1 pool and the dry shielding test room. The cross section of the beam hole on pool side and on room side are 30 x 30 cm² and 60 x 70 cm² respectively. A helium tank is positioned over the pool side end of the beam hole and a shielding door is over the room side end. The shielding door has a beam hole. The strength and characteristics of radiation are changed by moving the helium tank up or down, and inserting filters into the beam hole.

5.3.3 Gamma-ray Source Apparatus

The gamma-ray source apparatus is for gamma-ray experiments with radio-isotopes. It is composed of a device to put in and take out radio-isotope capsules, a store room of 12 radio-isotopes (50 curies maximum each), an activation device, gamma-ray irradiation device and rabbit tubes connecting them. The gamma-ray irradiation device is in the dry shielding test room, and the activation device is near the core (thermal flux is about 10^{10} n/cm²-sec). The others are in the reactor room. The irradiation device has a collimator provided to let the gamma-rays subtend in the range of 0° - 45°. The centerline of the flux can also be changed in direction up to 20° from the horizontal.

5.3.4 Instrument Bridge

Measuring instruments are suspended from the instrument bridge, similarly to the pool, and controlled from the measuring room. The position of the instruments is indicated with an accuracy of 10 mm.

Shielding experiments with JRR-4 are expected to start in April, 1965, after measuring the characteristics of the reactor.

6. CONCLUSION

An outline of the shielding investigations in Japan is given in the foregoing pages. For details of each contribution in this summary report, communication with the research workers is invited for clarifying any ambiguities that may be found. The Shielding Laboratory of JAERI will be pleased to transmit such communications from inquirers.

The editorial staff of this compilation was composed of M. Shindo, S. Miyasaka, Y. Furuta and A. Tsuruo of the Shielding Laboratory of JAERI, and I. Kataoka and T. Fuse of the Ship Research Institute.

REFERENCES

- 1) S. Miyasaka, Y. Furuta, A. Tsuruo, K. Tamura and Y. Kanemori: Preprint of 3rd National Nuclear Congress (1962)
- 2) K. Tamura, Y. Kanemori and Y. Furuta: Preprint of 3rd National Nuclear Congress (1962)
- 3) F. S. Kirn, J. Kennedy and H. O. Wyckoff: Radiology, 63, 94 (1954)
- 4) K. Tamura, A. Tsuruo and Y. Furuta: Preprint of 3rd Meeting of Reactor Physics (1963)
- 5) A. Tsuruo and T. Toyota: Preprint of 5-th Japan Conf. on Radio-isotope (1963)
- 6) S. Miyasaka, Y. Furuta, A. Tsuruo, K. Tamura and Y. Kanemori: Preprint of 3rd National Nuclear Congress (1962)
- 7) H. Mochizuki, Y. Tanaka, Y. Higashihara, N. Nagato and K. Yori-hisa: J. of Atomic Energy Soc. of Japan, 4, 448 (1962)
- 8) H. Mochizuki, Y. Tanaka, Y. Higashihara and K. Nagato: J. of Atomic Energy Soc. of Japan, 4, 703 (1962)
- 9) H. Mochizuki and Y. Tanaka: Nuclear Engineering, 9, 54 (1963) The Industrial Daily News Co.
- 10) M. H. Kalos: NDA-5607 (1956)
- 11) I. Umeda: Preprint of 5-th Japan Conf. on Radio-isotope (1963)
- 12) S. Nakata, I. Kataoka, K. Takeuchi and Y. Furuta: Preprint of 2nd National Nuclear Congress (1961)
- 13) S. Suguri, Y. Furuta and Y. Tanaka: JAERI 5002 (1960)
- 14) K. Ishimatsu: J. of Atomic Energy Soc. of Japan, 4, 175 (1962)
- 15) M. Hattori, T. Nagahara and S. Oku: Private communication
- 16) M. Nakata, T. Fuse and K. Takeuchi: J. of the Transportation Technical Research Institute, 11 (1961)
- 17) M. Nakata: J. of Non-Destructive Inspection, 10 (1961)
- 18) T. Hyodo: N.S.E., 12, 178 (1962)
- 19) H. Fujita, K. Kobayashi and T. Hyodo: To be published
- 20) K. Mizukami, T. Matsumoto and T. Hyodo: To be published
- 21) A. Tsuruo and T. Miyazaki: Preprint of 2nd National Nuclear Congress (1961)
- 22) Y. Odan, M. Kato and O. Sato: Preprint of 4-th Japan Conf. on Radio-isotope (1961)
- 23) Y. Furuta and A. Tsuruo: Private communication
- 24) Y. Furuta and Y. Kanemori: Private communication
- 25) K. Takumi and H. Mitsui: Private communication
- 26) H. Mochizuki et al.: To be published
- 27) M. Sakuta: Transaction of the Architectural Institute of Japan, No. 88 (1963)
- 28) Y. Fukushima and H. Yamaki: Preprint of Annual Meeting of the Atomic Energy Society of Japan (1963)
- 29) H. Mochizuki et al.: To be published
- 30) A. Tomabechi and T. Ishii: Preprint of Annual Meeting of the Atomic Energy Society of Japan (1963)
- 31) K. Ishimatsu: J. of Atomic Energy Soc. of Japan, 4, 24 (1962)
- 32) T. Hyodo and F. Makino: The Memoirs of the Faculty of Eng., Kyoto Univ., 24, part 2 (1962)
- 33) F. C. Maienschein: ORNL-1142 (1952)

- 34) Y. Furuta and S. Kinbara: Preprint of 16-th Annual Meeting of Physical Society of Japan (1961)
- 35) Y. Furuta: Private communication
- 36) Y. Furuta and S. Kinbara: To be published
- 37) T. Fuse: To be published
- 38) Y. Furuta and T. Fuse: Private communication
- 39) T. Fuse: JAERI 1015 (1961)
- 40) R. B. Owen: AERE-EL/R-2712 (1958)
- 41) H. Ishikawa, T. Asaoka and H. Sasakura: JAERI 1002 (1960)
- 42) A. Tsuruo and M. Sibuya: The 3rd Japan Conf. on Radio-isotope (1959)
- 43) M. J. Berger and J. Dogget: J. of Res. of NBS, 56, 89 (1956)
- 44) Y. Toyoda and T. Kondo: The 1st National Nuclear Congress (1960)
- 45) I. Umeda: To be published
- 46) Y. Nakano: Japan Nuclear Ship Research Association 42 (1963)
- 47) T. Ishi, T. Sekine and K. Ono: Seminar on Codes for Reactor Computations at Vienna (1960)
- 48) A. Tsuruo: Japan Nuclear Ship Research Association 33 (1962)
- 49) I. Kataoka: To be presented at 3rd Geneva Conf.
- 50) I. Kataoka and K. Takeuchi: To be presented at the Annual Meeting of the Atomic Energy Society of Japan (1964)
- 51) I. Kataoka and K. Takeuchi: Preprint of Annual Meeting of the Atomic Energy Society of Japan (1963)
- 52) H. Ono and A. Tsuruo: Preprint of 3rd National Nuclear Congress (1962)
- 53) A. Tsuruo: Preprint of Annual Meeting of the Atomic Energy Society of Japan (1963)
- 54) I. Kataoka: Preprint of 2nd National Nuclear Congress (1961)
- 55) C. Cooper et al.: 2nd Geneva Conf. P/84 (1958)
- 56) N. Hokkyo and M. Kitazume: AEC-tr-5077 (1960)
- 57) C. E. Iliffe: J. of Inst. Mech. Eng., Nuclear Energy Symposium (1956)
- 58) H. Mochizuki and Y. Tanaka: J. of Atomic Energy Soc. of Japan, 4, 448 (1962)
- 59) M. H. Kalos: NDA-5607 (1956)
- 60) D. L. Broder et al.: Atomnaya Energiya, 12, 30 (1962)
- 61) M. Kitazume: Preprint of 3rd Meeting of Reactor Physics of Atomic Energy Society of Japan (1962)
- 62) A. Tsuruo: J. of Atomic Energy Society of Japan, 6, No. 2 (1962)
- 63) M. Kitazume: Preprint of 3rd National Nuclear Congress (1962)
- 64) M. Shindo, A. Tsuruo and M. Kawabata: Preprint of Annual Meeting of Atomic Energy Society of Japan (1963)
- 65) M. Kitazume and T. Tagami: Preprint of 3rd National Nuclear Congress (1962)
- 66) M. Kitazume and T. Tagami: Preprint of Annual Meeting of the Atomic Energy Society of Japan (1963)
- 67) S. Tanaka, Y. Tanaka and K. Mori: Preprint of 1st National Nuclear Congress (1960)
- 68) A. Tsuruo: Preprint of 1st National Nuclear Congress (1960)
- 69) M. Sakuta, H. Maeda and M. Yamamoto: Nuclear Engineering, 8, 8, 27 (1960) The Industrial Daily News Co.
- 70) N. Okajima: Private communication
- 71) Report of Nuclear Ship Research Association of Japan, 21 (1961), 33 (1962), 45 (1963)

- 72) I. Kataoka, T. Yoshioka and K. Odawara: Preprint of Annual Meeting of the Atomic Energy Society of Japan (1963)
- 73) Private communication
- 74) Private communication
- 75) Private communication

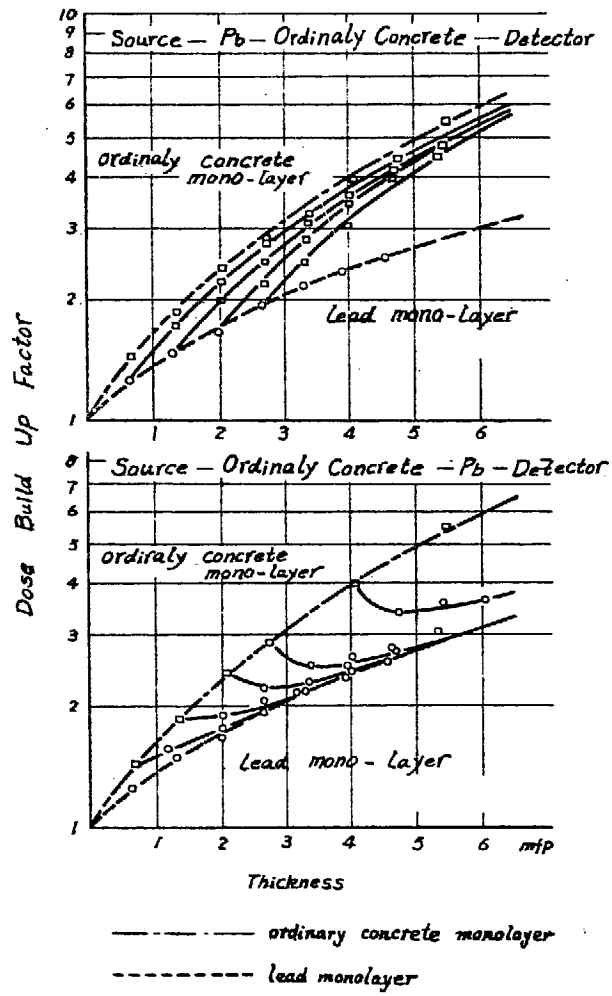


Fig. 1 Dose buildup factors of multi-layers (for lead and ordinary concrete)

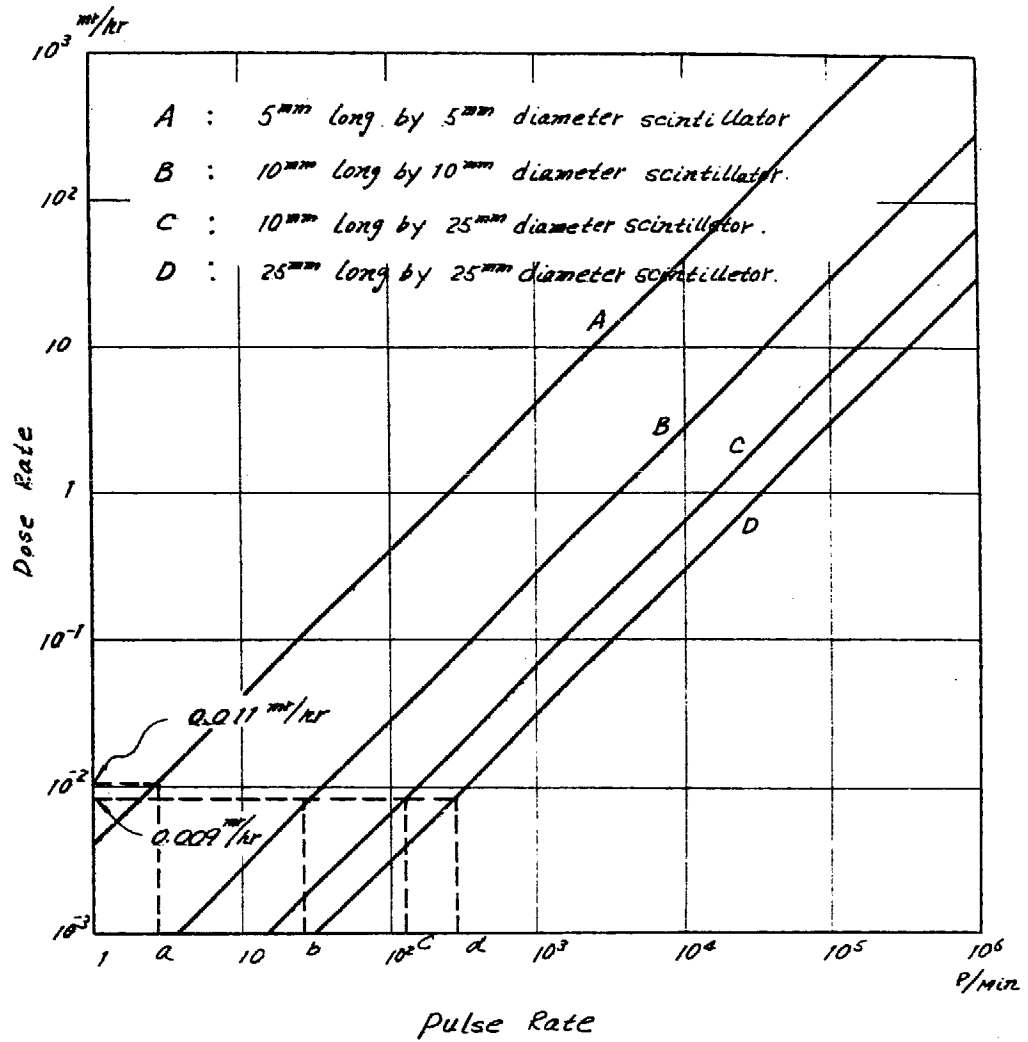
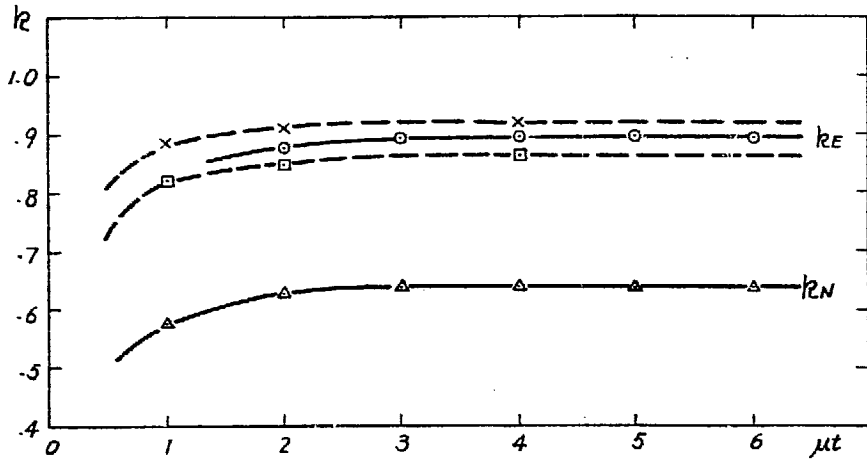
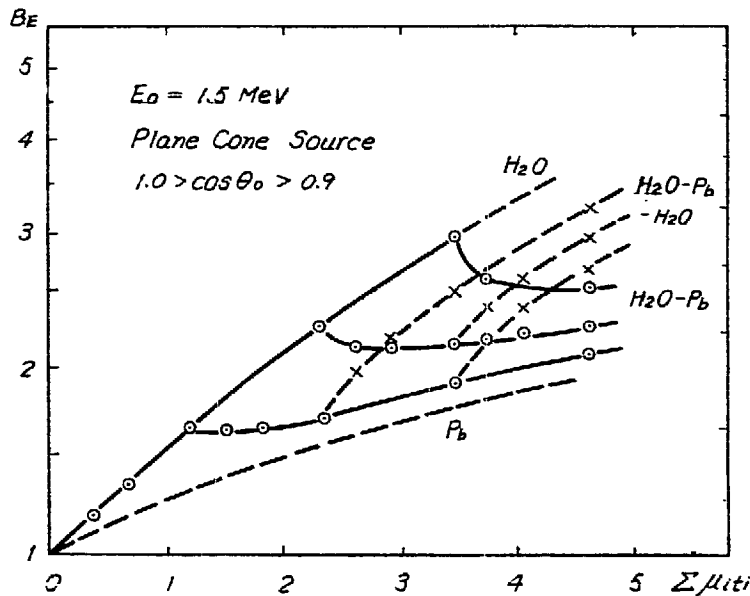


Fig. 2 Sensitivity of gamma-ray pulse dosimeter
Symbols of a, b, c, and d shows the pulse rates obtained for the natural background radiations with respective scintillators at the same point.



- △— Number flux k_N for Semi infinite Quadrant of Al $E_0 = 1.25$ MeV (Tsuruo)
- Energy flux k_E for Semi infinite Quadrant of Al $E_0 = 1.25$ MeV (Tsuruo)
- ×— Energy flux k_E for Slab of H_2O $E_0 = 4$ MeV (Berger)
- Energy flux k_E for Slab of Fe $E_0 = 1$ MeV (Berger)

Fig. 3 Monte carlo calculation of the ratio of buildup factor for a corner of semi-infinite Quadrant $B(\infty/4)$ to that for a semi-infinite medium $B(\infty/2)$, plane monidirectional source, incident angle 45° . $k = B(\infty/4) - 1 / B(\infty/2) - 1$



- $H_2O - Pb - H_2O$ Multiple Layer
- ×— $H_2O - Pb$ Multiple Layer

Source Energy $E_0 = 1.5$ MeV

Angular distribution of the source $1.0 > \cos \theta_0 > 0.9$

Fig. 4 Energy buildup factor for multiple layer by the response matrix method.

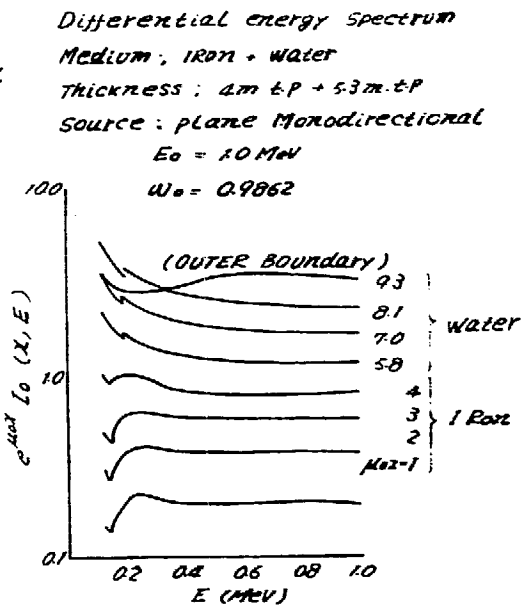
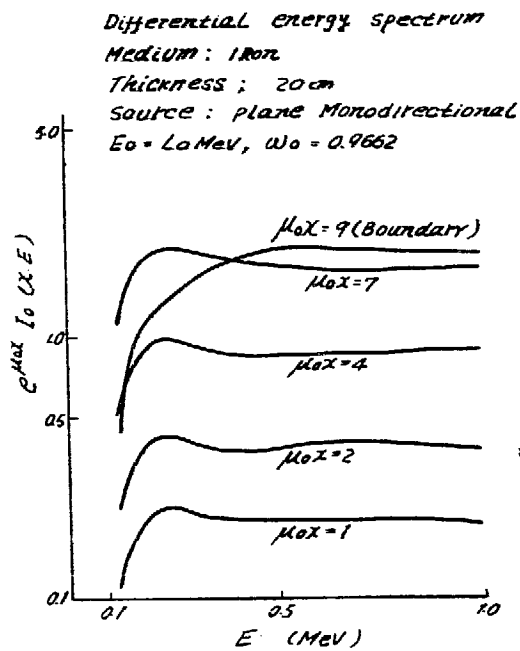
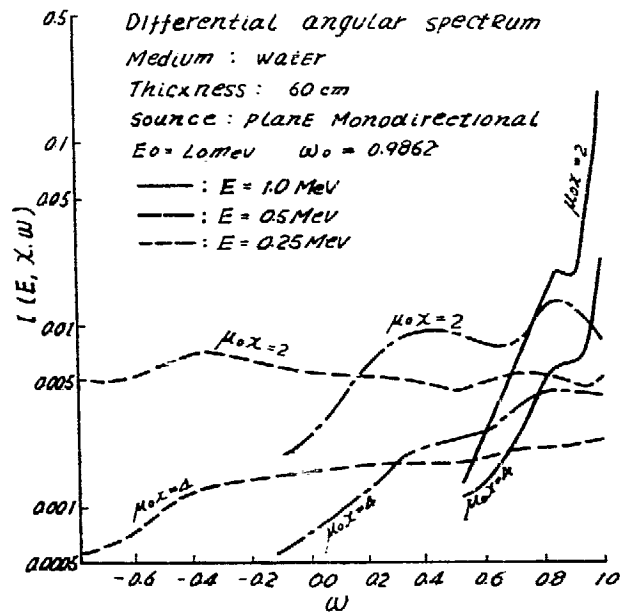
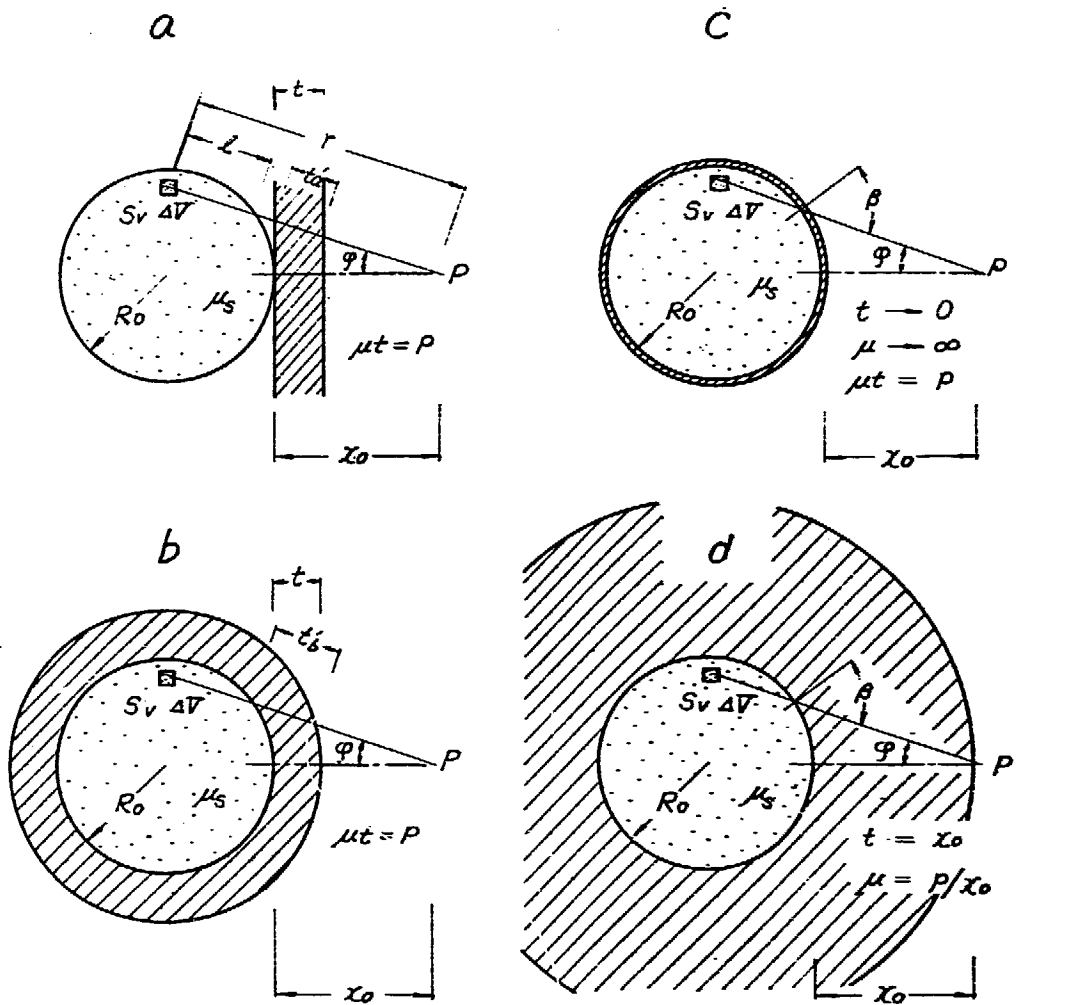


Fig. 5 Calculated gamma-ray spectrum of energy flux in the finite slab shield by EOS-1 code.



- a Slab shield
- b. Shell shield, slab thickness t is smaller than x_0 the distance between source surface and observation point.
- c. Shell shield, the thickness t is infinite thin and attenuation coefficient μ is infinite large so as to $\mu t = p$ is finite constant.
- d. Shell shield, slab thickness t is equal to x_0 , the distance between source surface and observation point.
- and $\phi_c \leq \phi_b \leq \phi_d \leq \phi_a$ for unscattered flux at point P.

Fig. 6 Typical shapes of shield for spherical source and cylindrical source.

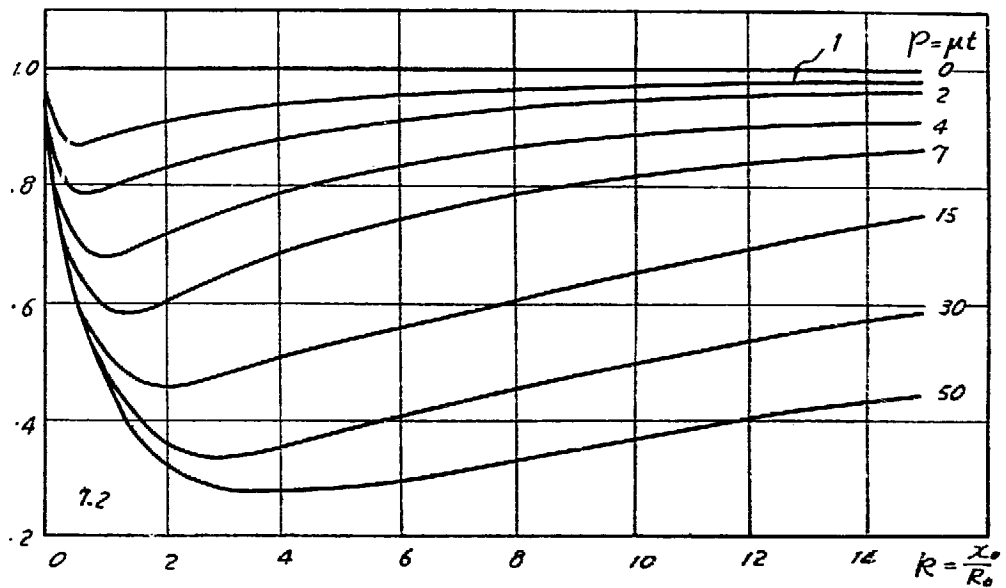
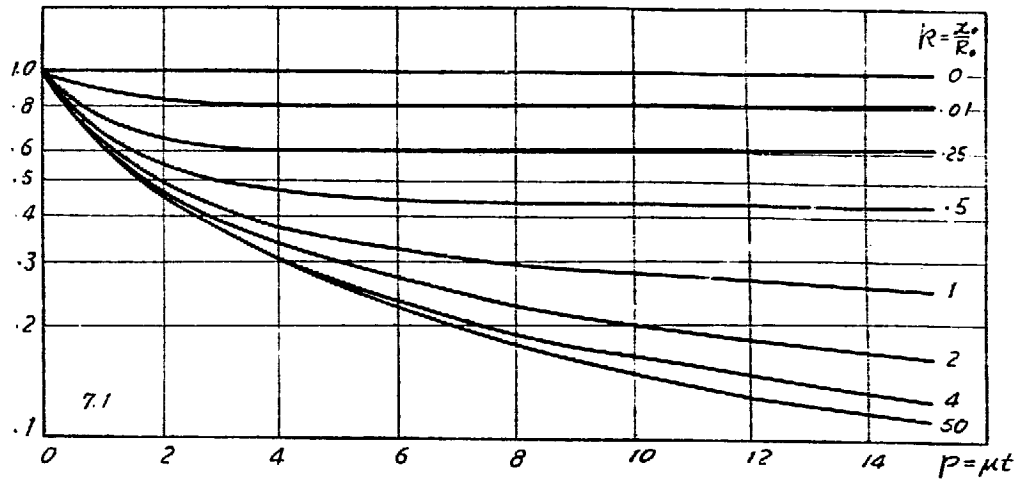


Fig. 7 Geometrical effect function for shell shield of spherical shield

$$S_1 \left(\frac{x_0}{R_0}, \mu t \right) = \phi_c / \phi_a$$

$$S_1 \left(\frac{x_0}{R_0}, \mu t \right) = \phi_d / \phi_a$$

$$\text{and } S_1(k, p) = \int_{u_0}^1 e^{-p \sec \beta} du / \int_{u_0}^1 e^{-p/u} du$$

$$S_2(k, p) = \int_{u_0}^1 e^{-p M_1(x, u) / x} du / \int_{u_0}^1 e^{-p/u} du$$

where $\phi_a, \phi_c, \phi_d, \sec \beta, u = \cos \varphi, p = \mu t, k = x_0 / R_0,$ are illustrated in Fig. 4

1. No. 1 pool
2. No. 2 pool
3. Gate
4. Lid tank
5. Control and measuring rooms
6. Basement floor
7. 1st floor
8. 2nd floor
9. Reactor bridge
10. Reactor core
11. Instrument bridge (pool.)
12. Instrument shaft
13. Instrument bridge (lid tank)
14. Converter
15. Thermal column
16. Dry shielding test room
17. Loading dock
18. 15/5 ton crane
19. Cat walk
20. Hatch
21. Laboratory

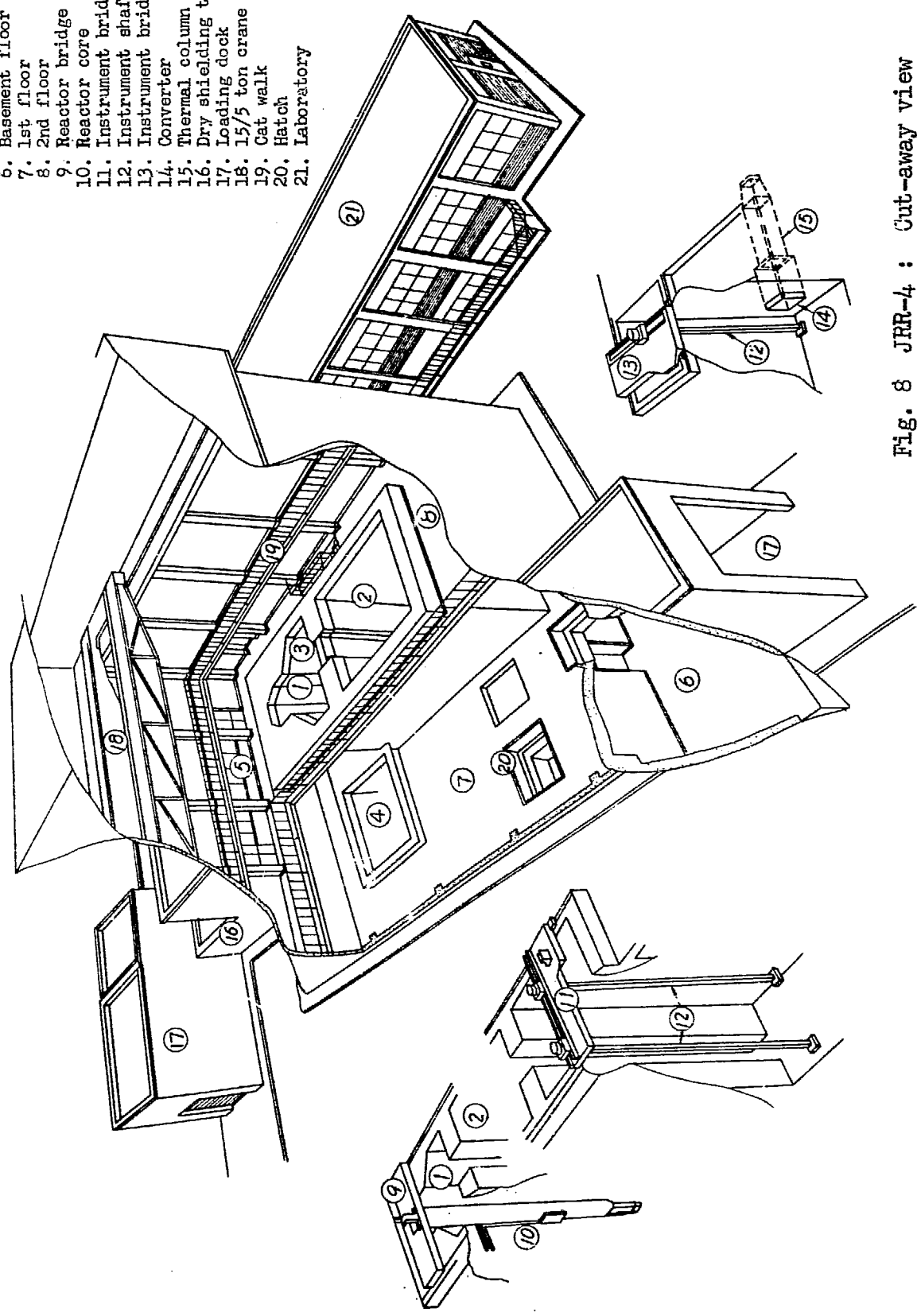
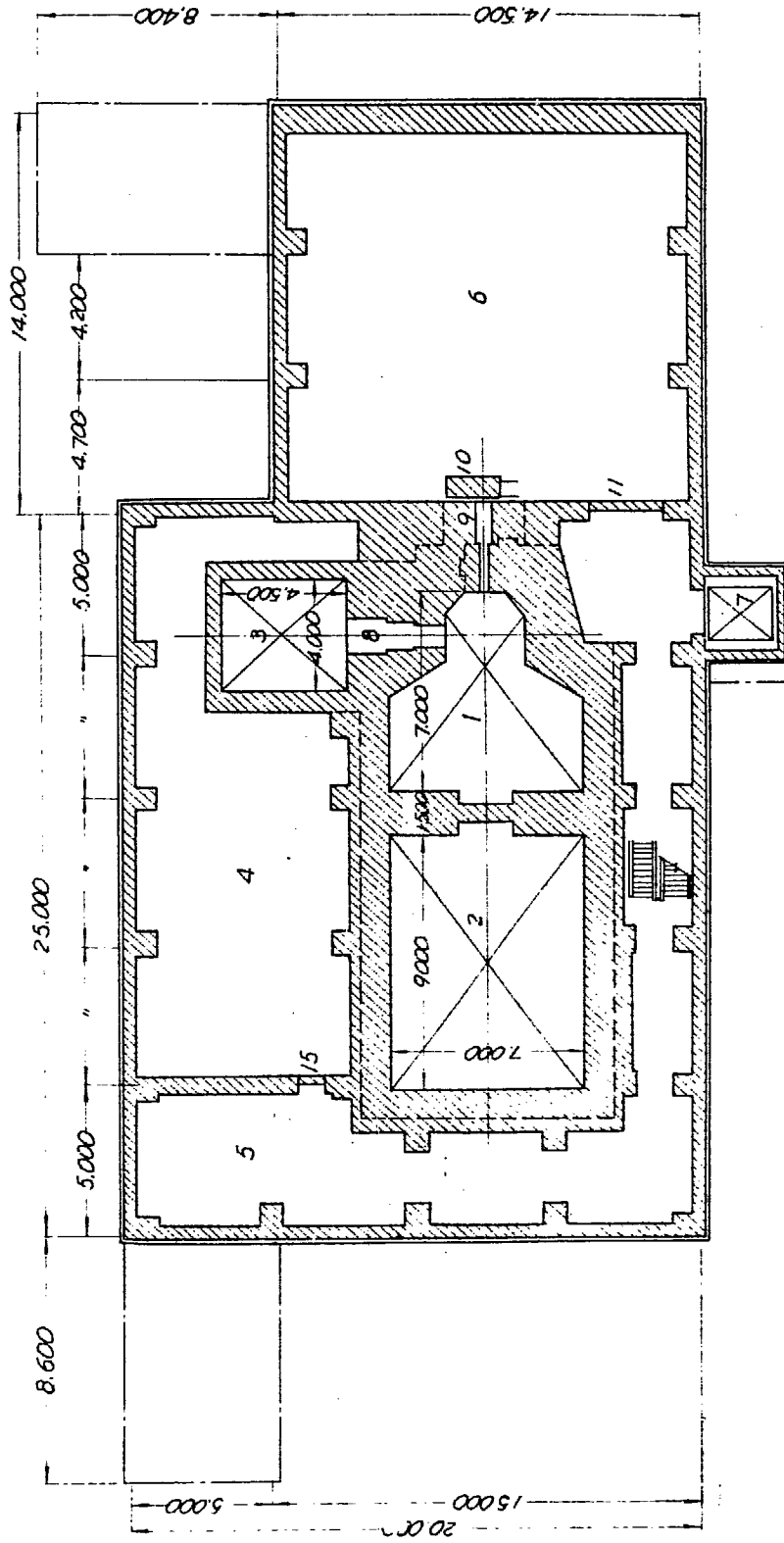


Fig. 8 JRR-4 : Cut-away view



- 1. No. 1 pool
- 2. No. 2 pool
- 3. Lid tank
- 4. Machinery room
- 5. Store room
- 6. Dry shielding test room
- 7. Elevator shaft
- 8. Thermal column
- 9. Beam hole
- 10. Shielding door
- 11. Shielded door

Fig. 9 JRR-1: Horizontal section of reactor

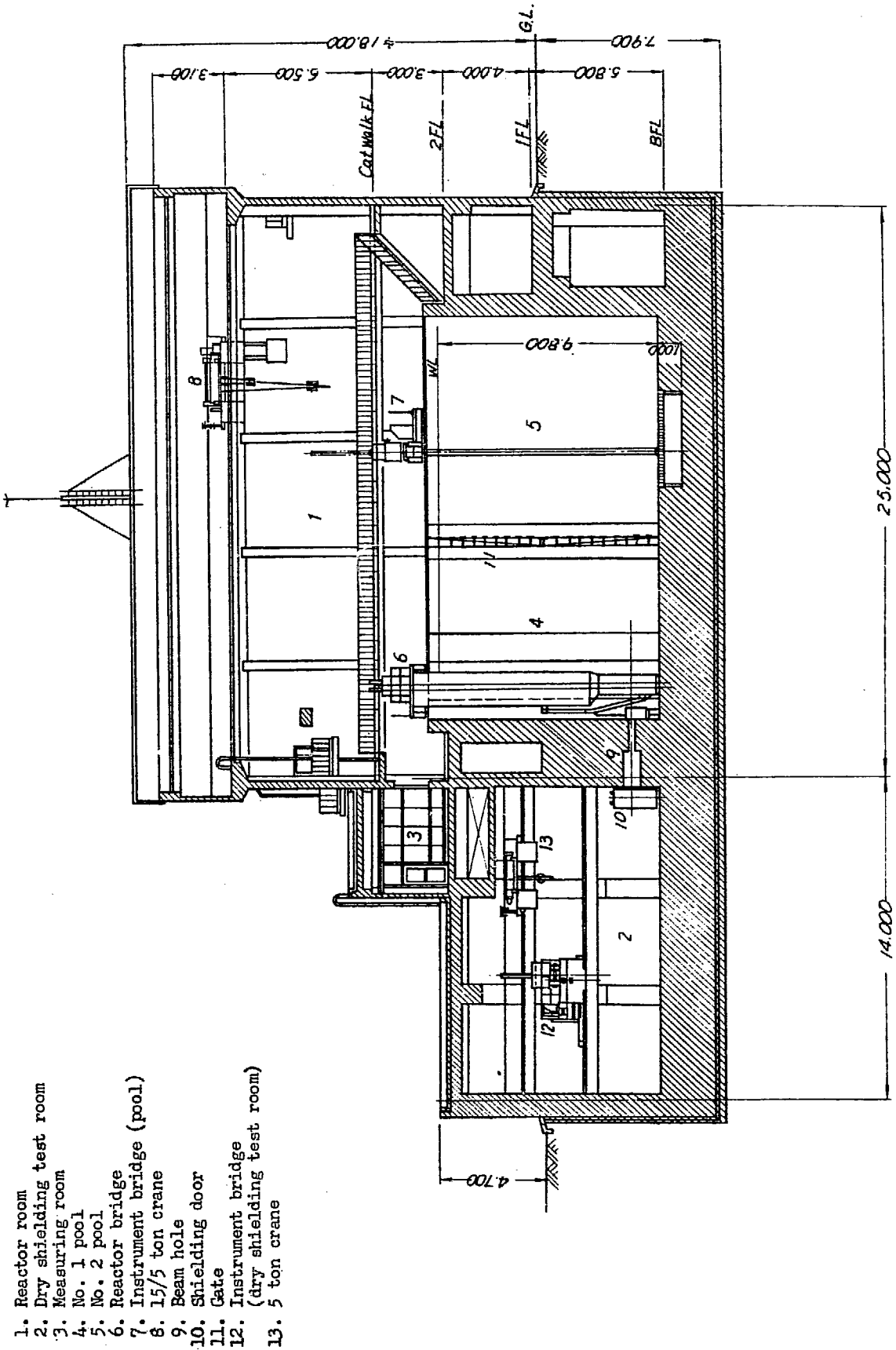


Fig. 10 JRR-4 : Vertical section of reactor